UKACC International Conference on Control 2012
Cardiff, UK, 3-5 September 2012

Robust adaptive fault estimation for a commercial aircraft oscillatory fault scenario

Xiaoyu Sun, Ron J Patton
Department of Engineering, University of Hull
Hull, UK
X.Sun@2009.hull.ac.uk; r.j.patton@hull.ac.uk

Philippe Goupil
Flight Control System Department, Airbus
Toulouse, France
philippe.goupil@airbus.com

Abstract— **A linear time invariant model-based robust fast adaptive fault estimator with unknown input decoupling is proposed to estimate aircraft elevator oscillatory faults. Since the robust fast adaptive fault estimator depends on system output error dynamics which are de-coupled from the unknown inputs (modeling uncertainty), the fault estimation signal generated by the designed fault estimator is robust to the estimated unknown inputs. To obtain a fast fault estimation speed, an adaptive fault estimator involves both proportional and integral components. A Lyapunov stability analysis of the robust fast adaptive fault estimator is given and the fault estimator dynamic response is achieved by pole assignment in subregions realized by LMIs. The proposed robust fast adaptive fault estimator is implemented on a high-fidelity nonlinear aircraft model to detect and estimate elevator actuator oscillatory faults.**

Keywords- adaptive fault estimator; unknown input ; fault estiamation ; linear matrix inequalities; Oscillatory Fault Case.

I. INTRODUCTION

The traditional approach to detecting and isolating faults in a flight control system makes use of hardware redundancy by a replication of hardware [1] (sensors, actuators or even flight control comp3ters). However, there is a growing interest in methods which do not require additional hardware redundancy, for easing the development of the future more sustainable aircraft (Cleaner, Quieter, Smarter and More Affordable). Highlighting the link between aircraft sustainability and fault detection, it can be demonstrated that improving the diagnosis performance in flight control systems allows the designers to optimize the aircraft structural design (resulting in weight saving), which in turn helps improve aircraft performance and to decrease its environmental footprint. Concretely, if the minimum detectable fault amplitude and/or the detection time can be decreased, the aircraft structural design will be improved and the aircraft will be made lighter [2].

As an alternative to hardware redundancy the model-based approach, often referred to as Fault Detection and Diagnosis (FDD) or Fault Detection and Isolation (FDI) makes use of analytical redundancy by generating redundant estimates of measured signals [3]. Although fault information generation via model-based FDD method for actuators (or sensors) generally increases the flight control system computational load, they can increase aircraft sustainability by improving fault diagnosis performance which leads to the possibility of optimizing aircraft structural design. All of which can help to achieve the challenges related to the "greening" of the aircraft. Model-based FDD has often been considered for fault detection, fault location and even diagnosis of fault severity in aircraft flight control systems [4, 5].

Many approaches to robust model-based FDD have been proposed in the past decades [4-8]. The major challenge is that the fault information signal should be robust to unknown inputs (UIs), used to represent a structured form of modelling uncertainty. To achieve the FDD robustness, different methods have been studied, e.g. the use of optimization methods [4], the unknown input observer (UIO) [6], the sliding mode observer [7] and geometric design approaches [8].

The method proposed in this paper is applied to a non-linear simulation of a generic aircraft provided by AIRBUS for a benchmark study within the ADDSAFE FP7 project [9, 10]. The benchmark is considered highly representative of the flight physics and aircraft handling qualities. One of the often considered fault scenarios is the oscillatory fault case (OFC) {sometimes referred to as the "oscillatory failure case"} which can be caused, for example by electronic system component faults. The moving flight surface of an aircraft can sometimes experience oscillation which may be generated in the servo-loop control, i.e. between the flight control computer (FCC) and the actual control surface itself. The spurious sinusoidal signals can propagate through the FCC and hence the control surface, as shown in Fig.1 [11]. As the fault is a local phenomenon within a single actuator, it only has an impact on one control surface. This OFC scenario has been studied by [7, 11] to detect the OFC fault.

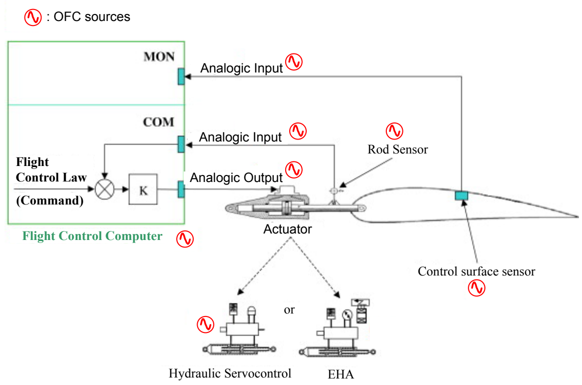

Figure 1. OFC source location in the control loop

A well-known method for estimating fault signals uses a combination of proportional and integral action within a full

The authors acknowledge funding from the EU FP7 project FP7-233815, Advanced Fault Diagnosis for Sustainable Flight Guidance and Control (ADDSAFE). Xiaoyu Sun has also been supported via a PhD scholarship in the Department of Engineering, Hull University.

order identity observer [12]. However, these authors did not consider the robustness of the fault estimation to modeling uncertainty. The current work provides an extension to the work of [12] by using a UIO to take into account the effects of so-called UI signals. The estimator design problem is divided into two stages of (i) UI distribution matrix estimation followed by (ii) the actual fault estimation, with inclusion of proportional (not only integral) action to enhance to the fault estimation speed. The proposed approach is termed a Robust Fast Adaptive Fault Estimator (RFAFE) based on a combination of the UIO proposed in [6] and the Fast Adaptive Fault Estimator of [12]. The RFAFE is applied to the problem of estimating the oscillatory fault signal acting on an elevator of the ADDSAFE benchmark system. The benefit of the proposed RFAFE is that by making the output error of the observer insensitive to modelling uncertainty the fault estimation robustness is improved.

The robustness of the fault estimation is defined to be the degree of comparison between the sensitivity of the estimation to the fault compared with the sensitivity to modeling uncertainty. The fault estimation must be accurate with relative insensitivity to modelling uncertainty.

The nonlinear aircraft model is not available for publication due to confidential issues. However, the results in this paper have been generated by applying the new RFAFE fault estimation strategy to the fully non-linear aircraft system dynamics via the ADDSAFE project. Following a procedure in [6] the structure of the modelling uncertainty inherent between the nonlinear and linear time invariant (LTI) aircraft models are considered as UI terms in the linear models used for the development of the fault estimator. In stage (i) of the RFAFE design, the influences of the UIs are estimated by estimating the "directions" (i.e. distributions) of these terms into the state space model as described in [3, 13]. In stage (ii) the fault estimator is then applied directly to the fault residual signal. This study focuses on the problem of detecting OFC fault activity in one elevator actuator (referred to as the "left" actuator).

The structure of the paper is as follows: In Section II, the proposed RFAFE design is formulated. In Section III, the LTI longitudinal aircraft model dynamics including elevator model dynamics are constructed. The RFAFE method is applied to the ADDSAFE benchmark system in Section IV to estimate various OFC faults. The conclusion is given in Section V.

II. ROUBST ADAPTIVE FAULT ESTIMATION THEORY

A. Fast adaptive fault estimation with UI decoupling

A LTI system considering actuator faults (all sensors are assumed to be fault-free) and with modeling uncertainty, represented by the UI term $Ed(t)$ is represented as:

$$\left.\begin{aligned}\dot{x}(t) &= A\,x(t) + Bu(t) + Ed(t) + F_a f_a\,(t)\\ y(t) &= C\,x(t)\end{aligned}\right\} \tag{1}$$

where $x \in \Re^n$ denotes the time-varying system state vector, $u \in \Re^r$ and $y \in \Re^m$ denote the input and measurement vectors, respectively and $d \in \Re^p$ is a vector of UIs. $f_a \in \Re^l$ represents a vector of time-varying actuator faults. A, B, C are known system matrices with appropriate dimensions. The matrix $E \in \Re^{n\times q}$ represents the distribution matrix for the UIs. The columns of the matrix $F_a \in \Re^{n\times l}$ denote the independent fault directions. It is thus considered that both E and F_a act as system inputs.

Following [3], a functional observer is constructed as:

$$\left.\begin{aligned}\dot{z}(t) &= Nz(t) + TBu(t) + Ky(t) + TF_a\hat{f}_a(t)\\ \hat{x}(t) &= z(t) + Hy(t)\end{aligned}\right\} \tag{2}$$

where $\hat{x} \in \Re^n$ is the estimated state vector and $z \in \Re^n$ is the observer state vector, and N , T, K and H are design matrices.

Definition 1: Observer (2) is defined as a *robust fast adaptive fault estimator (RFAFE)* for the system (1), if its state and fault estimation errors $e_x = x - \hat{x}$ and $e_f = f_a - \hat{f}_a$ approach zero asymptomatically, in the presence of the system UIs and faults.

Assuming that E is known, the estimation error dynamics are governed by:

$$\begin{aligned}\dot{e}_x(t) = (A - HCA - K_1C)e_x(t)&\\ +[N - (A - HCA - K_1C)]z(t)&\\ +[K_2 - (A - HCA - K_1C)H]y(t)&\\ +[T - (I - HC)]Bu(t)&\\ +(HC - I)Ed(t) + TF_a e_f(t)&\end{aligned} \tag{3}$$

where

$$K = K_1 + K_2 \tag{4}$$

If the following relations are satisfied:

$$(HC - I)E = 0 \tag{5}$$

$$T = I - HC \tag{6}$$

$$N = A - HCA - K_1C = A_1 - K_1C \tag{7}$$

$$K_2 = NH \tag{8}$$

The state estimation error is then refined as:

$$\dot{e}_x(t) = Ne_x(t) + TF_a e_f(t) \tag{9}$$

$$e_y(t) = ce_x(t) \tag{10}$$

$$r(t) = y(t) - C\hat{x}(t) = Ce_x(t) = e_y(t) \tag{11}$$

Furthermore, if all eigenvalues of N are stable, $r(t)$ will approach zero asymptotically, i.e. $\hat{x} \to x$ and $\hat{f}_a \to f_a$. The observer (2) is an UI decoupling *fast adaptive fault estimator* for the system (1) when conditions (5) – (8) are satisfied. Therefore, this RFAFE design involves the solution of (4) to (8) whilst placing all the eigenvalues of the system matrix N to be stable. Meanwhile, N , T , K and H in (2) are designed to achieve the required fault estimation performance.

A particular solution to (5) can be calculated as follows:

$$H = E(CE)^{+} \tag{12}$$

where: $(CE)^{+} = [(CE)^{T}CE)]^{-1}(CE)^{T}$ denotes the Moore-Penrose pseudo-inverse.

Theorem 1. The necessary and sufficient conditions for the existence of RFAFE of system (1) are [3, 12]:

(i) $rank(CE) = rank(E)$
(ii) $rank(CF_a) = rank(F_a)$
(iii) $rank([E\ F_a] = q + l$
(iv) (C, A_1) is a detectable pair

Remark 1: Condition (i) denotes that the maximum number of independent UIs cannot be larger than the maximum number of independent measurements, i.e. the necessary condition for UI decoupling in the state estimation error dynamics is $rank(E) \leq m$. If this condition is not satisfied, a rank approximation via a matrix E^{*} can be derived using Singular Value Decomposition (SVD) [14]. The details in [3] are addressed in Section B.

Remark 2: (ii) expresses that the maximum number of independent faults cannot be larger than the maximum number of independent measurements, i.e. the necessary condition for fault estimation in the states error dynamics is $rank(F_a) \leq m$.

Remark3: (iii) means that the UIs and faults are separable.

Remark 4: (iv) is equivalent to the following two equations.

(1) $rank\begin{bmatrix} sI - A & E \\ C & 0 \end{bmatrix} = n + rank(E)$

(2) $rank\begin{bmatrix} sI - A & B \\ C & 0 \end{bmatrix} = n + rank(B)$

Lemma 1 is used to verify the RFAFE existence conditions:

Lemma 1 [15]: Given a scalar $\theta > 0$ and a symmetric positive definite matrix P, the following inequality holds:

$$2x^{T}y \leq (1/\theta)(x^{T}Px) + \theta y^{T}P^{-1}y \quad x, y \in \Re^{n} \tag{13}$$

Assume that $\dot{f}_a \neq 0$, e.g. a sinusoidal perturbation (as required for the OFC fault case). The derivative of e_f is represented as:

$$\dot{e}_f = \dot{f}_a - \dot{\hat{f}}_a \tag{14}$$

The system error dynamics can be guaranteed by Theorem 2.

Theorem 2: With the assumption of Theorem 1, given the scalar $\alpha, \theta > 0$, if there exist symmetric positive definite matrices $P \in \Re^{n \times n}$, $Q \in \Re^{n \times n}$, $G \in \Re^{l \times l}$, and matrices $Y \in \Re^{n \times m}$, $N \in \Re^{l \times m}$ such that the following conditions hold.

$$\begin{bmatrix} PN + N^{T}P & -(1/\alpha)(N^{T}PTF_a) \\ * & -2(1/\alpha)(TF_a)^{T}PTF_a + (1/\alpha\theta)G \end{bmatrix} < 0 \tag{15}$$

$$(TF_a)^{T}P = MC \tag{16}$$

$*$ denotes the elements of a symmetric matrix, the UI decoupling fast adaptive fault estimator can be defined as:

$$\dot{\hat{f}}(t) = \Gamma M(\dot{r}(t) + \alpha r(t)) \tag{17}$$

(17) can be realized when $r(t)$ and e_f are uniformly bounded functions. $\Gamma \in \Re^{l \times l}$ is a symmetric positive definite learning rate matrix.

Proof: Consider the following Lyapunov function:

$$V(t) = e_x^{T}(t)Pe_x(t) + (1/\alpha)\, e_f^{T}(t)\Gamma^{-1}e_f(t) \tag{18}$$

Substituting (9) and (17) into (18), the derivative of $V(t)$ with respect to time is derived as:

$$\begin{aligned} \dot{V}(t) &= \dot{e}_x^{T}(t)Pe_x(t) + e_x^{T}(t)P\dot{e}_x^{T}(t) + 2(1/\alpha)\, e_f^{T}\Gamma^{-1}\dot{e}_f(t) \\ &= e_x^{T}(t)(PN + N^{T}P)e_x(t) + 2e_x^{T}(t)PTF_a e_f(t) \\ &\quad -2(1/\alpha)\, e_f^{T}(t)M(\dot{r}(t) + \sigma r(t)) \\ &\quad -2(1/\alpha)\, e_f^{T}(t)\Gamma^{-1}\dot{f}(t) \end{aligned} \tag{19}$$

Using (16), the term $-2(1/\alpha)\, e_f^{T}(t)M\big(\dot{r}(t) + \sigma r(t)\big)$ on the left hand side of (19) can be rewritten as:

$$\begin{aligned} &-2(1/\alpha)\, e_f^{T}(t)M\big(\dot{r}(t) + \sigma r(t)\big) \\ &\quad = -2(1/\alpha)\, e_f^{T}(t)(TF_a)^{T}P\big(\dot{e}_x(t) + \sigma e_x(t)\big) \end{aligned} \tag{20}$$

Substituting (9) and (20) into (19), $\dot{V}(t)$ can be formulated as:

$$\begin{aligned} \dot{V}(t) &= \dot{e}_x^{T}(t)(PN + N^{T}P)e_x(t) \\ &\quad -2(1/\alpha)\, e_f^{T}(t)(TF_a)^{T}PNe_x(t) \\ &\quad -2(1/\alpha)e_f^{T}(t)(TF_a)^{T}PTF_a e_f(t) \\ &\quad -2(1/\alpha)\, e_f^{T}(t)\Gamma^{-1}\dot{f}(t) \end{aligned} \tag{21}$$

By using Lemma 1, the following inequality can be obtained:

$$\begin{aligned} -2(1/\alpha)\, e_f^{T}(t)\Gamma^{-1}\dot{f}(t) &\leq (1/\alpha\theta)\, e_f^{T}(t)Ge_f(t) \\ &\quad +(\theta/\alpha)f_1^{2}\lambda_{max}(\Gamma^{-1}G^{-1}\Gamma^{-1}) \end{aligned} \tag{22}$$

Substituting (22) into (21), $\dot{V}(t)$ can be reformulated as:

$$\dot{V}(t) = \varphi^{T}(t)\,\Xi\,\varphi(t) + \delta \tag{23}$$

where

$$\varphi(t) = \begin{bmatrix} e_x(t) \\ e_f(t) \end{bmatrix}, \quad \delta = (\theta/\alpha)f_1^{2}\lambda_{max}(\Gamma^{-1}G^{-1}\Gamma^{-1}),$$

$$\Xi = \begin{bmatrix} PN + N^{T}P & -(1/\alpha)(N^{T}PTF_a) \\ * & -2(1/\alpha)(TF_a)^{T}PTF_a + (1/\alpha\theta)G \end{bmatrix}$$

TF_a is full column rank, under the condition of $\Xi < 0$, and $\epsilon = \lambda_{min}(-\Xi)$, then:

$$\dot{V}(t) < -\epsilon\|\varphi(t)\|^2 + \delta \quad (24)$$

for

$$\delta < \epsilon\|\varphi(t)\|^2 \quad (25)$$

Then, it follows that:

$$\dot{V}(t) < 0 \quad (26)$$

In terms of Lyapunov stability theory, (26) indicates that $e_x(t)$ and $e_f(t)$ converge to a small set of δ. This ends the proof.

If the fault signal is defined as:

$$f_a(t) = \begin{cases} 0 & t \in (0, \ t_f) \\ f_a(t) & t \in (t_f, \ \infty) \end{cases} \quad (27)$$

The fault estimation can be derived by (17) and given as:

$$\hat{f}(t) = \Gamma M(r(t) + \alpha \int_{tf}^{t} r(t)\, d\tau) \quad (28)$$

From (28), it can be seen that the fault estimation includes both proportional and integral parts. The proportional part enhances the fault estimator dynamic performance giving improved fault estimation speed.

Remark 5: Although inequality (15) can be solved easily via the Matlab LMI tool box, the simultaneous solution of (15) and (16) is difficult to achieve using functions in the LMI tool box. However, the problem can be solved by reformulating (16) into (29), which leads to the solution of optimization problem:

$$\begin{bmatrix} -\gamma I & (TF_a)^T P - MC \\ * & -\gamma I \end{bmatrix} < 0 \quad (29)$$

The RFAFE derivation is complete with proof of stability.

Apart from guaranteeing the observer stability, the observer dynamic response plays an important role in obtaining a qualified observer performance achieved by forcing the poles to lie within suitable complex plane subregions comprising either vertical strips, disks, conic sectors etc. (or their combinations) using LMIs optimization [16]. Here, disk and vertical strip LMI regions are employed as a further refinement to improve the fault estimator dynamics with LMIs defined as:

Definition 2: N is defined as in (7). Let $\mathcal{D}$ be an LMI subregion with characteristic function in the left hand side of the complex plane as a disk of radius r and centre $(-q, 0)$. Then there exists a symmetric matrix P such that:

$$\begin{pmatrix} -rP & qP + N^T P \\ * & -rP \end{pmatrix} < 0 \qquad P > 0 \quad (30)$$

Then, N is called $\mathcal{D}$–stable.

Definition 3: N is defined as in (7). Let $\mathcal{D}$ be a subregion which presents a ζ-stability region in the left-half plane. $\mathcal{D}$ is an LMI region with characteristic function, so that there exists a symmetric matrix P such that:

$$N^T P + PN + 2\zeta P < 0 \qquad P > 0 \quad (31)$$

Then, N is called $\mathcal{D}$ –stable. Fig. 2 shows the RFAFE poles assignment within an subregion $\mathcal{D}$ of an intersection between a specified disk and vertical strip by solving (30) & (31).

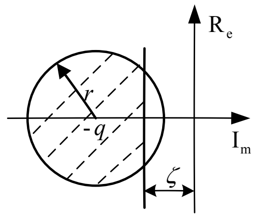

Figure 2. $\mathcal{D}$ subregion (hatched)

Consequently, a complete RFAFE with UI decoupling can be designed by solving (15), (29), (30), (31) and conditions (5)–(8) with the satisfaction of Theorem 2.

B. UI distribution matrix estimation

An augmented state observer is utilized to estimate the UI distribution matrix E. Assume that $d_1(t) = Ed(t)$ is a slowly time-varying vector, then the system model can be formulated in augmented form as [3, 13]:

$$\begin{bmatrix} \dot{x}(t) \\ \dot{d}(t) \end{bmatrix} = \begin{bmatrix} A & I \\ 0 & 0 \end{bmatrix} \begin{bmatrix} x(t) \\ d_1(t) \end{bmatrix} + \begin{bmatrix} B \\ 0 \end{bmatrix} u(t)$$

$$y(t) = [C_a \quad 0] \begin{bmatrix} x(t) \\ d_1(t) \end{bmatrix} \quad (32)$$

If the system inputs and outputs $\{u(t), y(t)\}$ are available, an observer based on the model presented by (32) can be used to estimate the $d_1(t)$ directly. The distribution matrix E is calculated as the ratio of the elements of $\hat{d}_1(t)$. The necessary condition for observability is given in Theorem 3:.

Theorem 3 The system (32) is observable if and only if the following conditions are satisfied [6].

(i) $rank(C) = n$
(ii) $rank(C, A)$ is a observable pair

Remark 6: Normally, the condition (i) could limit the application of this estimation approach. For a modern aircraft the states are available for measurement and this is also the case in the simulated non-linear system, so that the above observability and rank conditions are satisfied. Furthermore, the E estimation is a state space problem, and hence independent of any measurement restrictions.

For the RFEFA design, the necessary rank condition $rank(E) \leq m$ has been given in Theorem 1. If this condition is not satisfied, a sub-optimal matrix E^*can be computed as follows via an SVD expansion of E [3, 14]:

$$E = S\Sigma T^T \quad (33)$$

where:

$$\Sigma = \begin{bmatrix} diag\{\sigma_{1,\cdots,}\sigma_k\} & 0 \\ 0 & 0 \end{bmatrix} \quad (34)$$

S and T are orthogonal matrices, k is the rank, and $\sigma_{1,\ldots,}\sigma_k$ are the singular values of E , respectively. A low rank approximation for E by minimizing $\|E - E^*\|_F^2$ is given by:

$$E^* = S\hat{\Sigma}T^T \quad (35)$$

where

$$\hat{\Sigma} = \begin{bmatrix} diag\{0,\cdots,0,\sigma_{k-q,\cdots,}\sigma_k\} & 0 \\ 0 & 0 \end{bmatrix} \quad (36)$$

$q = rank(E^*) \leq m$ to satisfy Theorem 1 (for E^* instead of E).

III. LTI LONGITUDINAL AIRCRAFT MODEL DYNAMICS

The proposed RFAFE is implemented on a global longitudinal LTI model derived from the ADDSAFE benchmark system. Two parts constitute the global aircraft LTI model: one is the aircraft body axis LTI model derived from an LPV realization of the benchmark system obtained by choosing the trimming parameters given in TABLE I. The other part comprises the locally linear aircraft actuator models representing the right and left elevators on the aircraft tail surface. The linearized aircraft actuator models are generated for the same trimming parameters as the aircraft body axis LTI model.

TABLE I. TRIMMING POINTS FOR LONGITUDINAL AIRCRAFT LTI MODEL

Trimming parameter	value
MASS (Net mass in Kg)	200000
XG (Centre gravity of the aircraft in % / 100)	0.30
ZP (Altitude in feet)	20000
VC (Calibrate aircraft speed in kts)	290

The LTI local elevator model is represented by a first order system dynamic. For the longitudinal motion, the left and right elevator dynamics combined together have the structure:

$$\left.\begin{aligned} \dot{x}_a(t) &= A_a\, x_a(t) + B_a u_c(t) \\ y_a(t) &= C_a\, x_a(t) + D_a u_c(t) \end{aligned}\right\} \quad (37)$$

where $x_a(t) \in \Re^{2\times1}$ is the augmented state vector for both the left and right elevators. $u_c(t) \in \Re^{2\times1}$ is the vector of elevator control inputs (the actuator input signals fed from the FCC), y_a is the actuator output. A_a, B_a, C_a,D_a are corresponding system matrices with proper dimensions.

The LTI state space representation of the aircraft body axis dynamics can be expressed as:

$$\left.\begin{aligned} \dot{x}_b(t) &= A_b\, x_b(t) + B_u u_b(t) \\ y_b(t) &= C_b x_b(t) + D_u u_b(t) \end{aligned}\right\} \quad (38)$$

where $x_b = [V_{tas}, \alpha, q, \theta]$ and $y_b = [V_{tas}, \alpha, q, \theta]$ are the aircraft body axis states and outputs, respectively. u_b is equal to y_a. V_{tas} is the true air speed in m s^{-1}, α is the angle of attack in deg, q is the pitch rate in deg s^{-1}, θ is pitch angle in deg. A_b, B_b,C_b, D_b are the corresponding system matrices.

The complete LTI longitudinal motion model is formulated as:

$$\begin{bmatrix} \dot{x}_b(t) \\ \dot{x}_a(t) \end{bmatrix} = \begin{bmatrix} A_b & B_u C_a \\ 0 & A_a \end{bmatrix} \begin{bmatrix} x_b(t) \\ x_a(t) \end{bmatrix} + \begin{bmatrix} B_u D_a \\ B_a \end{bmatrix} u_c(t)$$

$$\begin{bmatrix} y_b(t) \\ y_a(t) \end{bmatrix} = \begin{bmatrix} C_b & D_u C_a \\ 0 & C_a \end{bmatrix} \begin{bmatrix} x_b(t) \\ x_a(t) \end{bmatrix} + \begin{bmatrix} D_u D_a \\ D_a \end{bmatrix} u_c(t) \quad (39)$$

(39) can be rewritten as:

$$\left.\begin{aligned} \dot{x}(t) &= A\, x(t) + Bu(t) \\ y(t) &= C\, x(t) + Du(t) \end{aligned}\right\} \quad (40)$$

LTI system (40) with UIs and faults can be presented as:

$$\left.\begin{aligned} \dot{x}(t) &= A\, x(t) + Bu(t) + Ed(t) + F_a f_a(t) \\ y(t) &= C\, x(t) + Du(t) \end{aligned}\right\} \quad (41)$$

IV. SIMULATION RESULTS

In this paper, the RFAFE design is implemented on a generic AIRBUS aircraft model to estimate the left elevator OFC fault. Two types of OFC are classified, the "liquid" and "solid" faults. The liquid fault is considered as an additive fault which adds to the control command inside the control loop. The solid fault is considered as a 'disconnected' fault which substitutes the control command completely inside the control loop. Both of these two OFC faults lead to the control surface performing with a spurious control command. In this project, the OFC faults are simulated as sinusoidal signals within a range of magnitudes and frequencies. The estimated OFC fault signals are normalized into the entire interval [0, 1] according to the elevator control surface deflection range of operation. In this simulation result section, the OFC signals 0.016 and 0.33 (in normalized units) are estimated to (a) demonstrate the effect that the OFC has on the elevator operation and (b) the effectiveness of the RFAFE design.

The first step of the RFAFE design is to estimate the UI distribution matrix as an off-line analysis. The modelling uncertainties between the nominal nonlinear aircraft model and the LTI aircraft longitudinal model are considered as UIs. The off-line design of the ASO for E estimation is made by running the ADDSAFE benchmark model. Six single fault-free cases (cruise phase, triggering of angle of attack protection, nose-up (abrupt longitudinal maneuver), triggering of pitch protection, coordinated turn and a "yaw-angle-mode" which roughly corresponds to an enhanced auto-pilot hold mode) are used to implement the estimation of the matrix E. The lower rank technique via the SVD approach is applied to post-process the modelling uncertainty data, so that condition (i) in Theorem 1 is satisfied. The second step of the RFAFE design is to construct the UI decoupling fast adaptive estimator in terms of the matrix E estimated in step 1. A set of conditions should be satisfied first and a group of LMIs should be solved as discussed in Section II. All the designs described in this paper use one aircraft longitudinal LTI model that corresponds to the operating point in TABLE I. The left elevator fault direction F_a is the first column of $B = [B_G, B_D]$, i.e. $F_a = B_G$.

Figs. 3&4 show the left elevator control surface position in two fault cases compared with the fault-free case, respectively. The control surface deflection is apparent, i.e. the OFC fault leads to unwanted control surface oscillation.

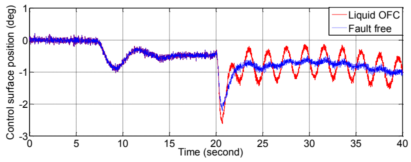

Figure 3. Left elevator control surface position (liquid OFC&fault-free cases)

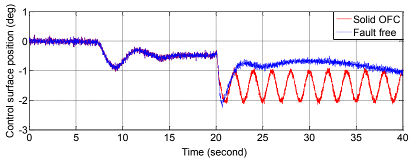

Figure 4. Left elevator control surface position (solid OFC & fault-free cases)

Fig. 3 corresponds to the liquid OFC. A sinusoidal signal is added to the normal control surface position. Fig. 4 shows the control surface movement trajectory is totally substituted by a sinusoidal signal for the solid OFC "disconnection" behaviour.

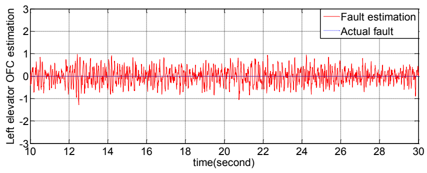

Figure 5. Left elevator fault estimation for the fault-free case

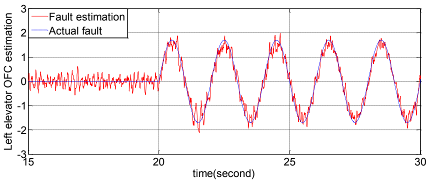

Figure 6. Left elevator fault estimation for the liquid OFC fault

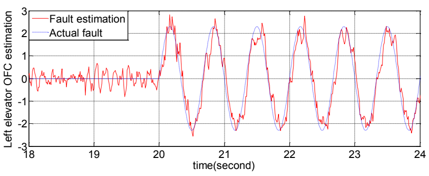

Figure 7. Left elevator fault estimation for solid OFC

Fig. 5 shows that in the fault-free case (left elevator) the estimates are in a noise level. In Figs. 6&7, the estimation of the so-called liquid OFC (0.016 OFC) and solid OFC (0.033 OFC) are shown, respectively. For each fault scenario, the faults occur at 20s and the fault estimation signals track the actual fault signals in magnitude and frequency.

The RFAFE design learning rate should be tuned to a suitable value to achieve accurate and fast fault estimation. It can also be seen that the fault estimation signal is not significantly affected by the modelling uncertainties, but is influenced by high frequency sensor noise. Hence, the fault estimation signal obtained is considered robust to modelling uncertainties.

V. CONCLUSION

In this paper, the RFAFE approach to fast fault estimation has been applied to an aircraft actuator OFC problem, taking into account modeling uncertainties through UI estimation. The UIs reflect the modelling mismatch between the linear and non-linear aircraft systems. The UI estimation considering a range of flight conditions provides a structured approach to robustness which leads to a robust fault estimation. The UI estimation with UI decoupling is utilized in the RFAFE design. The results show that the fault estimation signals track the actual fault signals accurately under both liquid and solid OFC faults in different magnitudes and frequencies, demonstrating the effectiveness and efficiency of the RFAFE method.

REFERENCES

[1] P. Goupil. AIRBUS State of the Art and Practices on FDI and FTC in Flight Control System. Control Engineering Practice 19 (2011), pp. 524-539 DOI information: 10.1016/j.conengprac.2010.12.009

[2] Goupil, P., Zolghadri, A., Gheorghe, A., Cieslak, J., Dayre, R. and Le-Berre H. Airbus efforts towards advanced fault diagnosis for flight control system actuators. 5th International Conference on Recent Advances in Aerospace Actuation Systems and Components (R3ASC'12), Toulouse, France, 13-14 June 2012.

[3] Chen, J. and R.J. Patton, *Robust model-based fault diagnosis for dynamic systems*. 1999, Norwell: Kluwer Academic Publishers

[4] Varga, A. Integrated algorithm for solving H_2-optimal fault detection and isolation problems. Proc.of Control and Fault-Tolerant Systems (SysTol). 2010.

[5] Chen, L. and R.J. Patton. Polytope LPV Fault Estimation for Non-Linear Flight Control. in Proceedings of the 18th IFAC World Congress. 2011.

[6] Chen, J., R.J. Patton, and H.Y. Zhang, Design of unknown input observers and robust fault detection filters. International Journal of Control, 1996. **63**(1): p. 85-105.

[7] Alwi, H. and C. Edwards. Oscillatory fault case detection for aircraft using an adaptive sliding mode differentiator scheme. in American Control Conference (ACC). 2011.

[8] Vanek, B., et al. Robust Model Matching for Geometric Fault Detection Filters: A Commercial Aircraft Example. 2011.

[9] DEIMOS Space, S.L.U, http://addsafe.deimos-space.com, 2011.

[10] Goupil, P. and A. Marcos. Advanced Diagnosis for Sustainable Flight Guidance and Control: the European ADDSAFE project. SAE 2011 AeroTech Congress & Exhibition October 18-21, 2011, Toulouse, France.

[11] Goupil, P., Oscillatory fault case detection in the A380 electrical flight control system by analytical redundancy. Control Engineering Practice, 2010. **18**(9): p. 1110-1119.

[12] Zhang, K., B. Jiang, and V. Cocquempot, *Adaptive observer-based fast fault estimation.* International Journal of Control Automation and Systems, 2008. **6**(3): p. 320.

[13] Patton, R.J. and J. Chen, Optimal unknown input distribution matrix selection in robust fault diagnosis. Automatica, 1993. **29**(4): p. 837-841.

[14] Golub, G.H. and C.F. Van Loan, *Matrix computations*. 1996, Baltimore and London: The Johns Hopkins University Press.

[15] Jiang, B., J.L. Wang, and Y.C. Soh, *An adaptive technique for robust diagnosis of faults with independent effects on system outputs.* International Journal of Control, 2002. **75**(11): p. 792-802.

[16] Chilali, M. and P. Gahinet, *H-infinity design with pole placement constraints: An LMI approach.* Automatic Control, IEEE Transactions on, 1996. **41**(3): p. 358-367.